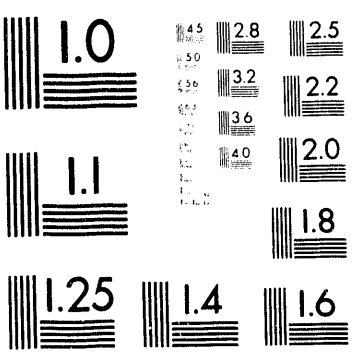
1.0
1.1
1.25
1.4
1.6
1.8
2.0
2.2
2.5
2.8
3.2
3.6
4.0
4.5
5.0
5.6

1 of 1

SLAC-PUB-6086
April 1993
(A)

# NUMERICAL SIMULATIONS OF INPUT AND OUTPUT COUPLERS FOR LINEAR ACCELERATOR STRUCTURES*

C.-K. Ng and K. Ko
Stanford Linear Accelerator Center
Stanford University, Stanford, CA 94309

## ABSTRACT

We present the numerical procedures involved in the design of coupler cavities for accelerator sections for linear colliders. The MAFIA code is used to simulate an X-band accelerator section with a symmetrical double-input coupler at each end. The transmission properties of the structure are calculated in the time domain and the dimensions of the coupler cavities are adjusted until the power coupling is optimized and frequency synchronism is obtained. We compare the performance of the symmetrical double-input design with that of the conventional single-input type by evaluating the field amplitude and phase asymmetries. We also evaluate the peak gradient in the coupler and discuss the implication of pulse rise time on dark current generation.

## 1. INTRODUCTION

At SLAC, we have an active program on the Next Linear Collider (NLC) R & D, and couplers are an important part of the accelerator structure work in this program. Indeed, the efficient delivery of power from RF sources such as klystrons to disk-loaded accelerator structures in linear colliders depends crucially on the coupler cavity. There are several requirements to be satisfied by such a cavity. First, it is to be well matched to the feeding waveguides (see Fig. 1) in order to couple the maximum amount of power into the structure to achieve the highest possible accelerating gradient. Second, it must be tuned to the synchronous frequency for the proper phase advance in the structure. Third, it must have minimal deleterious effect on the beam. Fourth, the couplers should ideally have surface fields no higher than the interior. These considerations, coupled with the fact that the geometry is intrinsically three-dimensional, make the design of the coupler cavity a nontrivial problem.

Previously, coupler cavities for disk-loaded accelerator structures have been designed following a set of procedures based on the Kyhl method[1]. It involves a sequence of experiments to determine the matching and tuning. Several iterations on actual prototypes may be needed before an optimal configuration can be obtained. The effort can be time-consuming and requires substantial empirical expertise. In this paper, we study an alternative approach by numerical simulation. We build a computer model that approximates closely the coupler cavity. Since changes in dimensions can be easily implemented on the computer, this approach offers a distinct advantage over cold tests in optimizing a design. Furthermore, valuable field information such as asymmetries and peak gradients, for example, is readily obtainable numerically, which otherwise would be difficult to measure experimentally. These advantages provide the motivation for our effort to develop an accurate and reliable computational procedure for matching and tuning this particular RF component.

In section 2, we describe the numerical model of the symmetrical double-input coupler using the MAFIA code[2]. Such a coupler has been incorporated into a 30-cavity section and operated up to 100 MV/m without evidence of breakdown. In section 3, the numerical procedure involved in matching and tuning the coupler is explained and the results are compared with experimental data in section 4. In section 5, we show the advantages of the symmetrical double-input design over the conventional single-input type in terms of field asymmetries. In section 6, we evaluate the peak gradients. The effect of pulse rise time is considered in section 7 where simulation results are presented to be corroborated with observations. We conclude with a summary in section 8.

* Work supported by Department of Energy, contract DE-AC03-76SF00515.



Contributed to the Computational Accelerator Conference (CAP93)
Pleasanton, CA, Feb 22-26, 1993

## 2. THE NUMERICAL MODEL

We model the symmetrical double-input coupler in the 30-cavity structure which was used in high power tests. Instead of all 30 cells, we simulate only a short section which is sufficient for matching the coupler and it is computationally more practical. Fig. 1 shows the mesh geometry we have constructed using MAFIA. It consists of two identical coupler cavities and two regular accelerator cavities. The coupler cavities are fed by WR90 rectangular waveguides through irises. Because the feeds are symmetrical, we only need to model one-quarter of the structure. The magnetic boundaries imposed at the two symmetry planes are consistent with the waveguide fields as well as the fields of the accelerating mode in the structure. The SLAC NLC operating frequency is chosen to be at X-band around 11.424 GHz. Accordingly, the dimensions of the regular cells in our model have been designed for that frequency at the $2\pi/3$ phase advance per cell. The dimensions of the couplers are different in order to fulfill the matching and tuning requirements described earlier.

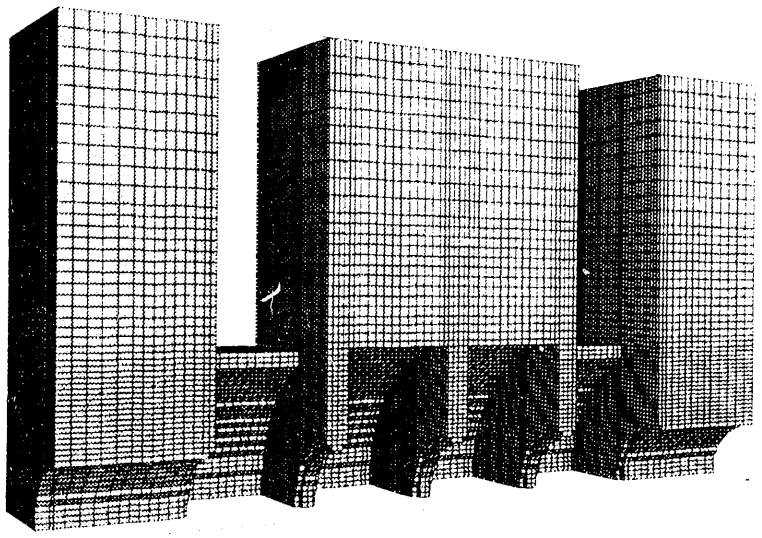

Fig. 1 MAFIA geometry for a 4-cell traveling wave section.

Given a coupler geometry, we perform a MAFIA simulation in the time domain. Power is fed continuously at the input waveguide port in the $TE_{10}$ mode at a particular frequency, starting with a smooth initial rise and reaching 1 watt at flat-top. The input power couples to the accelerating mode via the irises, propagates through the section and exits by way of the output coupler. The simulation extends over many filling times of the section until a traveling wave at steady-state is reached. At the end of the run, the reflection coefficient $S_{11}$ at the input waveguide port and the transmission coefficient $S_{21}$ at the output waveguide port are evaluated. In addition, the electric field on axis and in designated regions of interest is recorded for subsequent post-processing.

## 3. MATCHING AND TUNING OF COUPLER CAVITY

The cross-section of the coupler cavity is shown in Fig. 2(a). There are three dimensions to be determined: the coupler diameter, the iris aperture and its thickness. Assuming that the iris thickness is held fixed, the design program is then to choose the two remaining dimensions in such a way that the matching and tuning are optimal. These conditions are assessed as follows. As far as matching is concerned, we look for the minimum VSWR for the section. In the simulation, this corresponds to the smallest reflection coefficient $S_{11}$ at the input waveguide port. Fig. 3(a) shows the time history of $S_{11}$ for a typical case when the coupler is matched. We see that the steady-state can be reached after several filling times and the amount of reflection is quite acceptable (VSWR = 1.023 in this case). This is in contrast to an unmatched case as

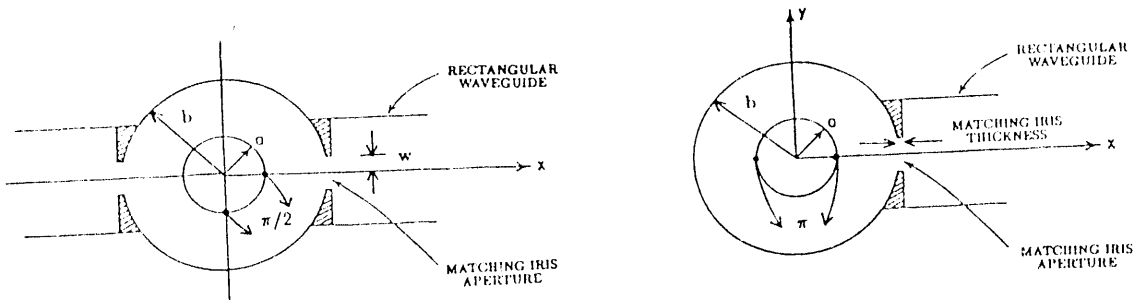


(a) (b)

Fig. 2 Schematics of (a) symmetrical double-input coupler; (b) single-input coupler.

shown in Fig. 3(b) which corresponds to a different set of coupler diameter and iris aperture dimensions. The VSWR = 1.475 is large compared with the matched case.

To evaluate tuning, we examine the amplitude and phase variations of the electric field on axis. One can write

$$E_T(z) = |E_T(z)|e^{-i\theta_T(z)}, \tag{1}$$

where the time variation has been left out. In the MAFIA run at steady-state, the electric field on axis along the structure is stored over several cycles which can be Fourier-analyzed to obtain $E_T$ and $\theta_T$. They are plotted in Figs. 4(a) and (b) for the same matched case mentioned above. The dashed lines mark the boundaries between cells. In both plots we see that the field is periodic in the regular cells. We also notice that it is symmetric about the center of the structure which should be the case when the couplers are nearly matched. In this case the fields look identical whether power is fed in at the input or output end. The phase advance in the two regular cells is 122°, close to the expected value of 120° at the driving frequency of 11.42 GHz. In the coupler cavities, the phase variation is zero across roughly half the cavity and totals to 62° for the whole cell. This suggests that the field in the half of the coupler cavity near the cut-off beam pipe is essentially a standing wave while the traveling wave in the other half advances by half the phase shift as compared to the regular cell. These results confirm earlier data from dielectric bead perturbation measurements[3]. As pointed out in that paper, the field amplitude and phase variations can provide a means by which the tuning of the coupler can be accurately determined. Numerically such a procedure is much easier to implement than in actual cold tests.

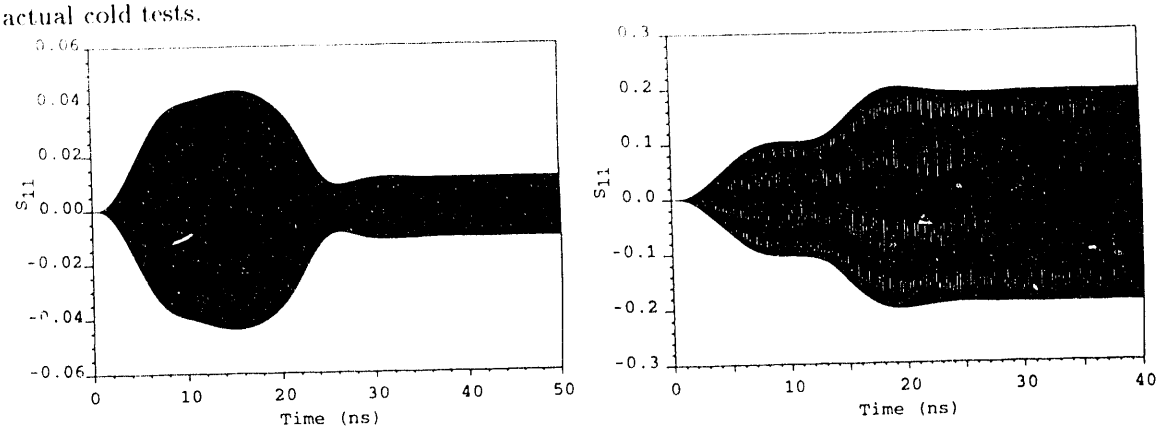


(a) (b)

Fig. 3 The reflection coefficient as a function of time for (a) a matched coupler; (b) an unmatched coupler.

For comparison, we show an unmatched case in Figs. 5(a) and (b). Here the field ampli-

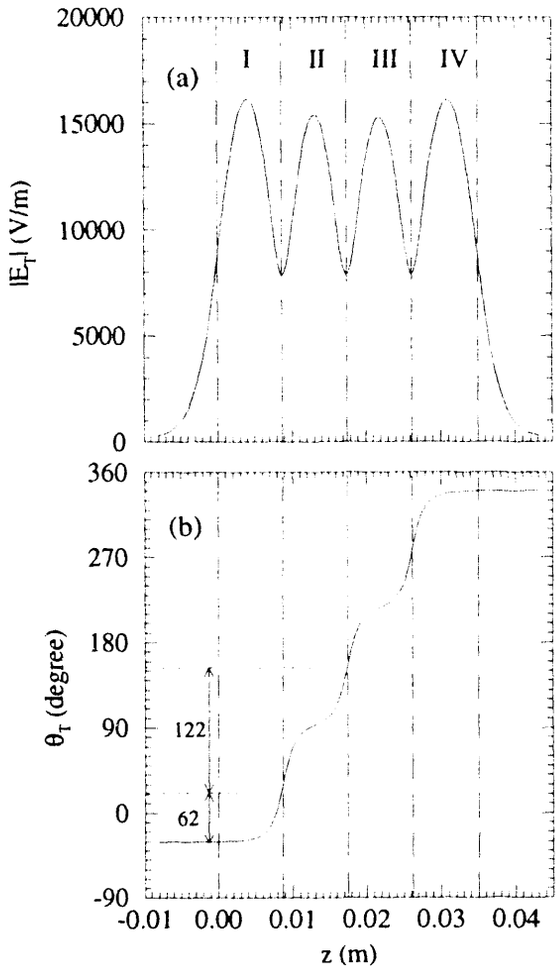


Fig. 4 Amplitude and phase variations for a matched coupler. Regions I, II & III, and IV are the input coupler cavity, the two structure cells and the output coupler cavity, respectively.

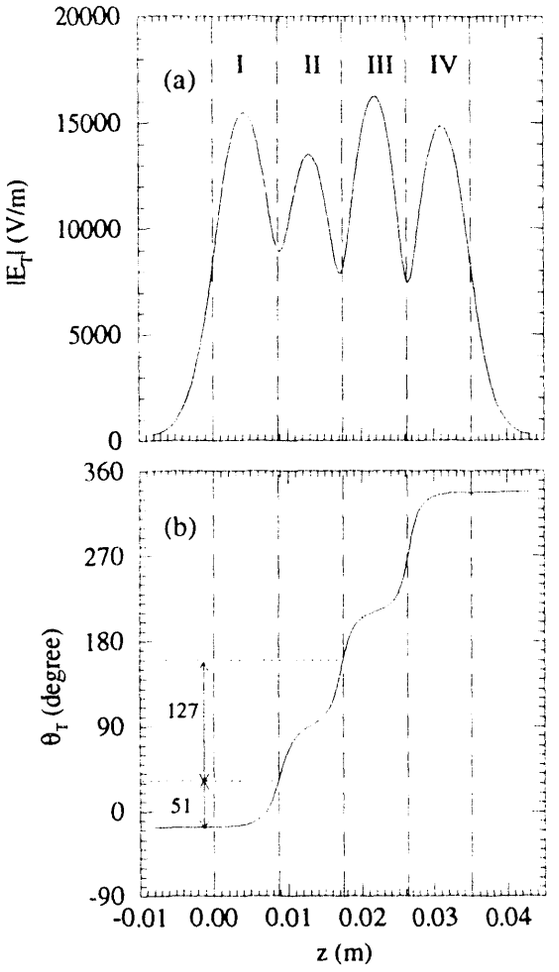


Fig. 5 Same as Fig. 4, but for an unmatched coupler with matching iris aperture increased by 0.006 inches.

tudes are irregular along the structure, quite different from the symmetric fields we saw earlier. Similarly, the phase advances in the coupler cavities and the regular cells deviate appreciably from the $\pi/3$ and the $2\pi/3$ values we expect to find in a tuned situation. The difference in dimensions in the coupler cavity from the matched case is an increase of 0.006 inches in the matching iris aperture.

## 4. COMPARISON BETWEEN SIMULATIONS AND EXPERIMENTS

In designing the symmetrical double-input coupler for the 30-cavity section, we performed a systematic numerical search for the optimal dimensions, using the matching and tuning conditions described above. We varied the cavity diameter and iris aperture, then calculated the VWSR and phase shifts in each iteration. Figs. 6(a) and (b) summarize the results. The driving frequency is again 11.42 GHz. The plots show, in effect, the sensitivity of matching and tuning to changes in coupler dimensions due to machining tolerances, for example. The perturbations ($\delta b$ and $\delta w$) are measured with respect to the dimensions ($b$ and $w$) for the matched case in which they are assumed to be zero. In Fig. 6(a) we find that the VSWR is much more sensitive to the coupler diameter than to the iris aperture. The same holds true for the phase shifts as

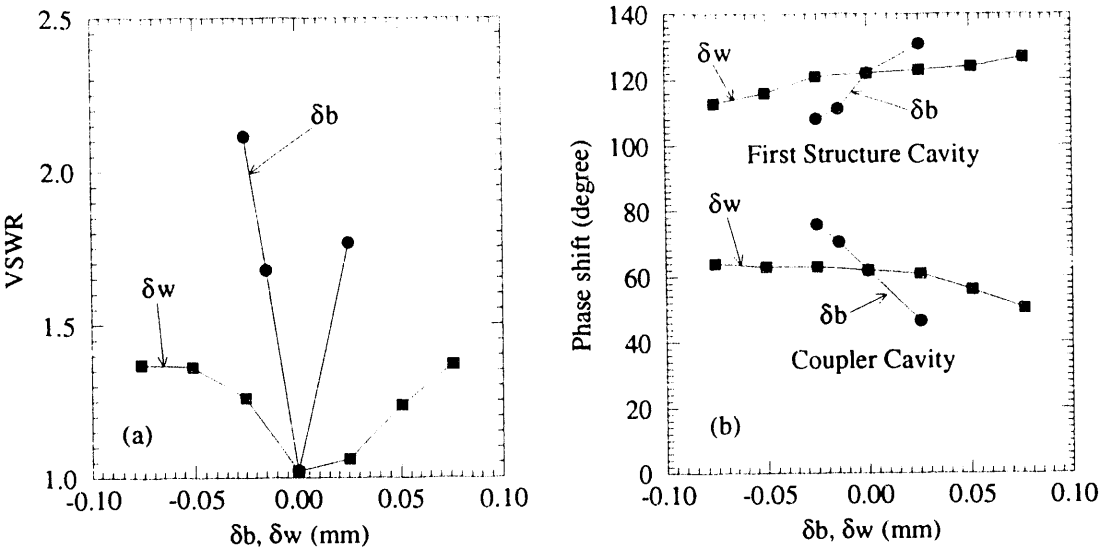


Fig. 6 The dependence of (a) VSWR; (b) phase shifts on the changes $\delta b$ in coupler radius $b$, and $\delta w$ in matching iris half aperture $w$.

shown in Fig. 6(b). We also note that about the optimum point, the dependence of the VSWR on slight changes in either dimensions is quadratic while that of the phase shifts is linear. Both are consistent with simple perturbation analysis.

With the coupler dimensions that we found for optimal matching and tuning, one can vary the frequency to explore the bandwidth. Fig. 7 shows a comparison of VSWR versus frequency between the MAFIA simulations and experiments[4]. Near the desired operating frequency of 11.424 GHz, the agreement is very good and the dimensions of the actual coupler are very close to those used in the MAFIA model. This is encouraging because it means that we can reasonably model the geometry for design purposes without expending an unrealistic amount of computational resources.

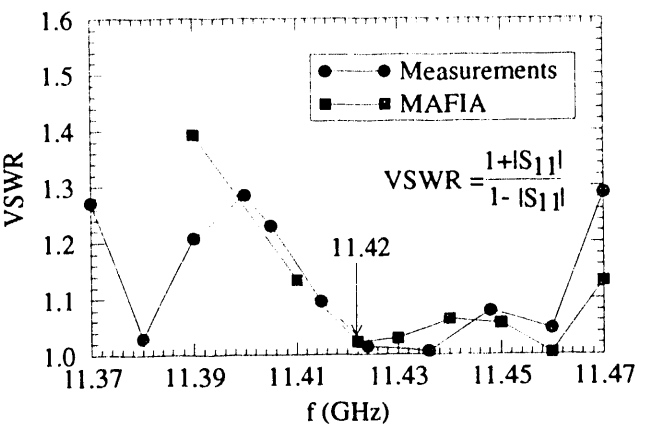


Fig. 7 VSWR versus frequency from MAFIA and measurements.

## 5. FIELD ASYMMETRIES IN COUPLERS

Conventional couplers are of the single-input type (see Fig. 2(b)) where power is fed in from a single waveguide. This configuration inherently introduces field asymmetries across the beam aperture in the form of a dipole component. The amplitude asymmetry leads to a shear force which spreads the bunch while the phase asymmetry results in a deflecting force on the bunch[5]. As discussed in Ref. 5, the amplitude asymmetry can be corrected by offsetting the cavity with

respect to the beam axis. The effect of phase asymmetry on the beam can be reduced by tilting the coupler cavity or by feeding successive sections from opposite sides.

In the symmetrical double-input coupler, assuming that the fields in both feeds are equal in amplitude and have the same phase, the dipole component is eliminated by virtue of symmetry. The remaining asymmetries are then due to the quadrupole component which can be measured by comparing fields at points 90° around the beam aperture (see Figs. 2(a) and (b)). In Table 1, we list the asymmetries for the single-input coupler before and after offset, and for the double-input coupler. The data for the single-input coupler are taken from Ref. 5 while those for the double-input are obtained from the MAFIA simulation of the matched case. We conclude from the results that the field asymmetry should be negligible near the beam axis in the double-input coupler. This makes it a superior design over previous single-input types. Presently, the input couplers for the 75 cm and 1.8 m structures being planned at SLAC have incorporated this double-input feature.

| Asymmetry | Single-input before offset | Single-input after offset | Double-input |
|---|---|---|---|
| $\frac{\Delta E}{E}\|_{\pi}$ | 10% | 0.1% | 0 |
| $\Delta\phi\|_{\pi}$ | 1.5° | 1.5° | 0 |
| $\frac{\Delta E}{E}\|_{\frac{\pi}{2}}$ | | | 6% |
| $\Delta\phi\|_{\frac{\pi}{2}}$ | | | 0.1° |

Table 1. Amplitude and phase asymmetries for single-input and double-input couplers. The designations "$\frac{\pi}{2}$" and "$\pi$" correspond to asymmetries shown in Fig. 2(a) and (b) at $r = a$.

## 6. PEAK FIELD GRADIENTS

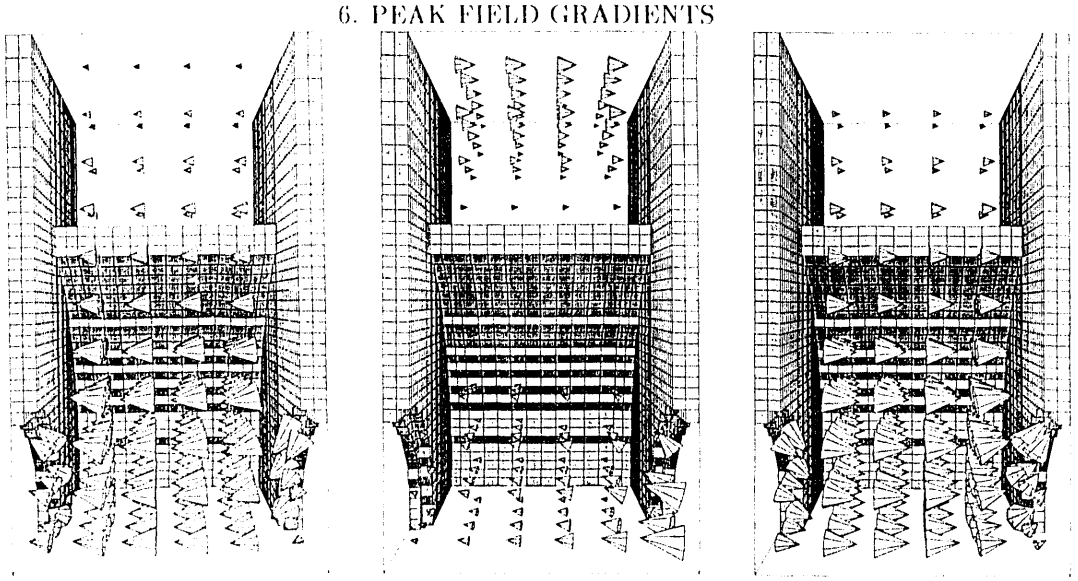

(a) (b) (c)

Fig. 8 Snapshots of electric fields in the input coupler at three different times. The left and right sides of the coupler are connected to the beam tube and the first structure cell, respectively. The peak gradients are (a) 235 MV/m; (b) 61 MV/m; (c) 239 MV/m.

One of the problems of common concern in accelerator structures is RF breakdown, which occurs when the peak electric field gradients reached in these structures exceed a certain critical value. At SLAC, an X-band 30-cavity accelerator section has been RF processed up to a stable accelerating field of about 100 MV/m, for a peak input power of 100 MW. While it is difficult to determine the locations of peak gradients experimentally, these can readily be obtained from our simulations.

Fig. 8 shows snapshots of the electric fields in the input coupler over approximately half a wave period at steady-state. We normalize the input power to 100 MW. The peak gradients are found to be 235, 61 and 239 MV/m for the three snapshots, respectively, and the maximum ($\sim$ 240 MV/m) is about a factor of 2.26 greater than the peak field along the axis. The maximum peak gradient occurs near the top part of the disk next to the first structure cell. Our result is in reasonable agreement with the measurement of the 30-cavity structure[6], where damage was seen near the top part of the coupler disk. Furthermore, the maximum peak gradient in the structure cell is found to be very close to that in the coupler from our suimulation.

## 7. PULSE RISE TIME EFFECT

A topic of great interest to accelerator designers is the generation of dark current by field emission at high gradient. Dark current observed in the high power tests of the 30-cavity traveling section was found to depend on the rise time of the RF pulse[7]. As the rise time got steeper, the resulting capture of electron increased. The effect was attributed to the upward frequency shift, caused by the rise time and resulting in a lower phase velocity. Here, we suggest a possible explanation by studying the space harmonic contents of the total field.

We have explored the effect of the pulse rise time with our MAFIA model. We scaled the rise times of the pulse to the filling time of our structure in the same ratios as those in the experiment, and hence chose 1.27 and 2.54 ns to correspond to the 10 and 20 ns cases that were measured. The fields in the half of the coupler which is traveling were Fourier-decomposed into their space harmonics. For a traveling wave, we can extend the analysis to a whole cell in the structure because of symmetry. Neglecting the time dependence, the peak electric field can be expressed as:

$$E_T(z) = \sum_{n=-\infty}^{\infty} C_n e^{-i\beta_n z}, \tag{2}$$

where the propagation constant for the $n$th space harmonic is $\beta_n = \beta_0(1+3n)$. For a structure with spatial period $D$ and operating at $2\pi/3$ mode, the synchronous component with phase velocity $c$ has a propagation constant $\beta_0 = 2\pi/3D$. The complex field $E_T(z)$ can be expressed in terms of its amplitude $|E_T(z)|$ and phase $\theta_T$ as in Eq. (1). Hence, if $|E_T(z)|$ and $\theta_T(z)$ are known by measurement or by numerical means, then $C_n$ can be determined as:

$$C_n = \frac{2}{D}\int_0^{\frac{D}{2}} |E_T(z)|\cos[\beta_n z - \theta_T(z)]\, dz. \tag{3}$$

It is convenient to normalize $|E_T(z)|$ to the maximum peak field $E_M$. Comparing Eqs. (1) and (2), the contributions of each space harmonic to the total field are given by the individual terms in the sum of the following equation:

$$|E_T(z)| = E_M \sum_{n=-\infty}^{\infty} b_n e^{-i[\beta_n z - \theta_T(z)]}, \tag{4}$$

where $b_n = C_n/E_M$. Furthermore, it can be shown easily that $\sum b_n = 1$. If the synchronous component has a phase velocity $c$, the phase velocities of the other space harmonics are given by $v_p = c/(1+3n)$, for $n = \pm 1, \pm 2, \ldots$. Therefore higher space harmonics have lower phase velocities.

In Fig. 9, we show the decomposition of the electric field along the axis at the end of the pulse into space harmonics across a cell for the two different rise times. The coefficients of $\{b_0, b_1, b_2, b_{-1}, b_{-2}\}$ for rise time 1.27 ns and 2.54 ns are $\{0.731, -0.076, 0.042, 0.369, -0.081\}$ and $\{0.741, -0.056, 0.026, 0.326, -0.051\}$, respectively. At the rise time of 1.27 ns, we see that the contributions of the higher order components ($n \neq 0$) are larger compared with those for the case with rise time of 2.54 ns. Therefore, electron capture by these lower phase velocity components is more important for short rise time. Of course, a realistic study of dark current

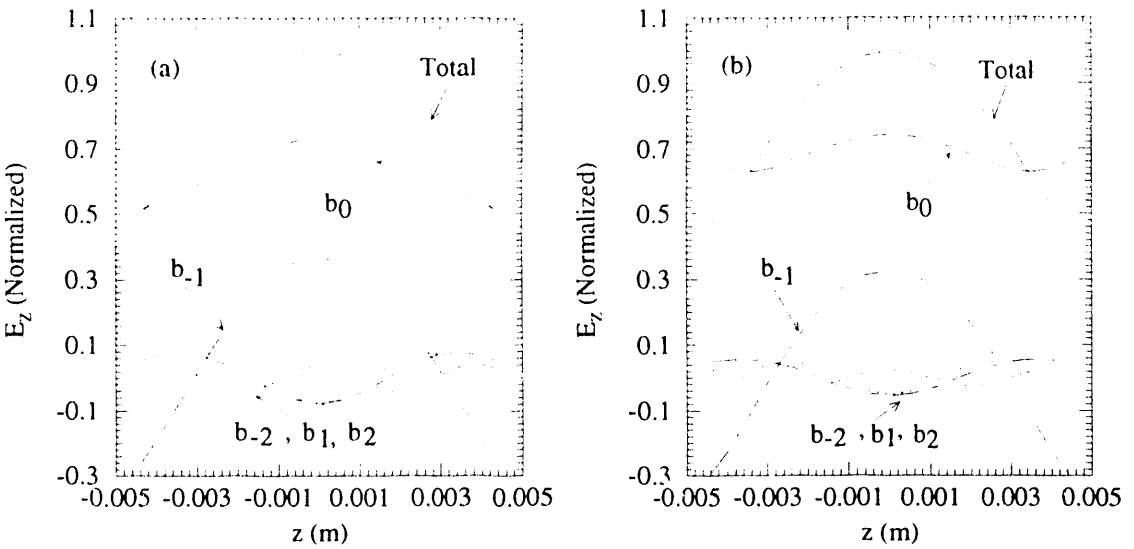


Fig. 9 Decomposition of the total field amplitude into space harmonics for rise time of (a) 1.27 ns; (b) 2.54 ns.

has to rely on particle simulation. Here, by simple Fourier analysis of the field amplitude, a qualitative understanding of dark current is obtained.

## 8. CONCLUSION

We have used MAFIA to simulate the symmetrical double-input coupler for an X-band accelerator structure. The numerical procedure for matching and tuning has been developed, and good agreement has been found between simulations and experiments. The advantage of the double-input over single-input geometry has been shown in terms of lower field amplitude and phase asymmetries, and the location of the peak gradient in the coupler cavity has been identified. Numerical results have also been presented to corroborate experimental observations on the dependence of captured dark current with RF pulse rise time. The present paper demonstrates that numerical simulations can provide very useful shortcut to cut-and-try prototyping in the design and analysis of linac coupler cavities.

## ACKNOWLEDGEMENTS

We wish to thank H. Deruyter for the cold test data and many fruitful discussions. We are grateful to G. Loew for a critical reading of the manuscript and numerous valuable suggestions, and R. Miller for very useful comments. We also acknowledge H. Hoag, J. W. Wang, J. Haimson, N. Kroll, E. Nelson and W. Herrmannsfeldt for their interest in the problem.

## REFERENCES

1. R. L. Kyhl, Impedance matching of disk loaded accelerator structures, unpublished (1976); E. Westbrook, Microwave impedance matching of feed waveguides to the disk-loaded accelerator structure operating in the $2\pi/3$ mode, SLAC-TN-63-103 (1963).
2. The MAFIA Collaboration, F. Ebeling et. al., MAFIA User Guide, 1992.
3. J. Haimson, Nucl. Instru. Meth., **39**, 13 (1966).
4. H. Deruyter et. al., Proceedings of Linac 92 Conference, p407, Ottawa, Canada, August, 1992.
5. G. A. Loew and R. B. Neal, Accelerator structures, in Linear Accelerators, p39-133, ed. P. M. Lapostolle and A. L. Septier, 1970.
6. J. W. Wang et. al., High-gradient studies on 11.4 GHz copper accelerator structures, SLAC-PUB-5900 (1992).
7. G. A. Loew, Review of studies on conventional linear colliders in the S- and X-band regime, SLAC-PUB-5844 (1992).

## DISCLAIMER

DATE

FILMED

11/10/93

END